Marine Geology 269 (2010) 46–60

Contents lists available at ScienceDirect

Marine Geology

journal homepage: www.elsevier.com/locate/margeo

# Late Holocene Evolution of the Mekong Subaqueous Delta, Southern Vietnam

Zuo Xue [a,*], J. Paul Liu [a,*], Dave DeMaster [a], Lap Van Nguyen [b], Thi Kim Oanh Ta [b]

[a] Department of Marine, Earth and Atmospheric Sciences, North Carolina State University, Raleigh, NC 27695, USA
[b] HoChiMinh City Institute of Resources Geography, Vietnam Academy of Science and Technology, Ho Chi Minh City, Vietnam

ARTICLE INFO

*Article history:*
Received 22 January 2009
Received in revised form 9 November 2009
Accepted 13 December 2009
Available online 23 December 2009

Communicated by J.T. Wells

*Keywords:*
subaqueous delta
mud wedge
delta evolution
sediment budget
South China Sea

ABSTRACT

As Asia's third largest river, with regard to sediment load, the Mekong River delivers approximately 160 million tons of sediment per year to the South China Sea. High-resolution seismic profiling and coring during 2006 and 2007 cruises revealed a low gradient, subaqueous delta system, up to 20 m thick, surrounding the modern Mekong River Delta (MRD) in the west of the South China Sea. Based on clinoform structure, grain size, $^{210}$Pb, AMS $^{14}$C, and $\delta^{13}$C results, the subaqueous delta is divided into four zones defined by different sedimentary processes and depositional features.

Over the past 3000 yr, the evolution of the MRD has shown a morphological asymmetry indicated by a large down-drift area and a rapid progradation around Cape Camau, ~200 km downstream from the river mouth. This asymmetric feature is consistent with increased wave influence. The strong southwestward coastal current, strengthened by the strong NE monsoon, plays an important role locally in longshore transport of resuspended sediments into the Gulf of Thailand.

A late Holocene sediment budget for the MRD has been determined, based on the area and thickness of deltaic sediment. Approximately 80% of Mekong delivered sediment has been trapped within the delta area, which, together with a falling sea-level, resulted in a rapidly prograding MRD over the past 3000 yr.



## 1. Introduction

Most of the world's deltaic systems began their formation between 7400 and 9500 cal yr BP as a result of decelerating sea-level rise (Stanley and Warne, 1994). These deltaic systems are characterized by different stratigraphy controlled by variations in relative sea level, fluvial inputs, marine dynamics, morphology, and tectonics. Conceptual processes-based models for deltaic deposition include: 1) river-dominated/influenced, such as the Mississippi, Yellow, and Po deltas, 2) wave-dominated/influenced, such as the Nile and Danube deltas, 3) tide-dominated/influenced, such as the Amazon, Yangtze, and Fly deltas (Galloway, 1975), and 4) deltas dominated by the combination of the former three processes, such as the Mekong Delta (Ta et al., 2002a,b). The evolution of a deltaic system is a non-steady process and is usually characterized by lobe switching, such as in the Mississippi (Roberts, 1997, 1998) and Po deltas (Correggiari et al., 2005), and even changes of dominant process, such as in the Mekong Delta (Ta et al., 2002a).

As part of the prograding depositional units of the deltaic systems, subaqueous deltas and clinoform structures have been documented in numerous deltaic systems including the Amazon (Nittrouer et al., 1986, 1996), Yellow (Liu et al., 2004, 2007a), Yangtze (Chen et al., 2000; Liu et al., 2007b), Po/Adriatic Sea (Cattaneo et al., 2003), Ganges-Brahmaputra (Kuehl et al., 1997; Goodbred and Kuehl, 1999, 2000), and Fly River/Gulf of Papua (Walsh et al., 2004; Slingerland et al., 2008). Late Quaternary sediment budgets have been established, based on the volume estimation of these subaqueous deltas and clinoform structures. Although historically the term “clinoform” has referred to the foreset part of a deltaic system, recent usage of the term refers to the topset–foreset–bottomset morphology of deltaic systems. The term “compound-clinoform” has been proposed to describe a subaerial/subaqueous delta couplet (Nittrouer et al., 1996; Swenson, 2005). Determined by multiple factors such as marine hydrodynamics, fluvial sediment inputs, eustatic sea level, and subsidence, the development and character of subaqueous deltas vary among different locations. In general, energetic marine environments, such as the Amazon Shelf, Gulf of Bengal, or Gulf of Papua are ideal for subaqueous delta development, whereas low energy environments, such as the Gulf of Mexico are less suited for development of such a feature (Swenson, 2005).

Studies of the sedimentation processes on the continental shelf off the Mekong River Delta (MRD) are limited. Seismic and sediment core studies only have been conducted either along the continental shelf edge (Schimanski and Stattegger, 2005) or to the south around the Sunda Shelf, where the paleo-shoreline was located during the Last Glacial Maximum (LGM) (Hanebuth et al., 2000, 2002, 2003, 2009; Hanebuth and Stattegger, 2004). This paper will present the results of a seismic and sediment core field study of the MRD's coastal area between 2006 and 2007, with specific interests focused on the morphology and sedimentatary processes of the subaqueous delta.

* Corresponding authors. Tel.: +1 919 515 7767; fax: +1 919 515 7802.
*E-mail addresses:* zxue@ncsu.edu (Z. Xue), jpliu@ncsu.edu (J.P. Liu).

0025-3227/$ – see front matter © 2009 Elsevier B.V. All rights reserved.
doi:10.1016/j.margeo.2009.12.005

## 2. The study area

### 2.1. The Mekong River and Delta

The Mekong River originates in the Tibetan Plateau, runs through China, Myanmar, Thailand, Lao PDR, Cambodia, and finally enters the South China Sea in southern Vietnam (Fig. 1). The total length of the Mekong River is about 4750 km and approximately half of it is in China's Yunnan province, locally known as the Lancang River. The Lower Mekong River region (Cambodia, Lao PDR, Thailand and Vietnam) has a population of 60 million, the majority of which depend on the aquatic resources provided by the river basin. The Mekong River watershed has an area of 832,000 km$^2$ (HYDROSHEDS v2.01, World Wildlife Fund, US). Annual water discharge of the Mekong River is $\sim 470 \times 10^9$ m$^3$ and the estimated annual sediment flux is ~160 million tons (Milliman and Syvitski, 1992). Compared with other large rivers, the Mekong River has a smaller drainage area than the Yangtze, Mississippi, or Ganges–Brahmaputra Rivers, but its sediment yield is about twice that of the Mississippi and nearly equal to that of the Yangtze. The estuarine area of Mekong River exhibits a funnel-like shape and is dominated by large tides with a maximum range of 3.2 m and average tide of 2.2 m (Wolanski et al., 1996).

The MRD is a wide, low-lying delta with an area of 49,500 km$^2$ (Le et al., 2007). The delta plain is the third largest in the world (Coleman and Roberts, 1989), 50% greater than the Yangtze delta, and is only exceeded by the Amazon and the Ganges–Brahmaputra deltas. With fast economic development in the Lower Mekong region, infrastructure (mainly dams and reservoirs upstream and artificial dykes in the delta plain), deforestation, and shrimp farms are dramatically changing the Mekong River's water and sediment discharge from source to sink.

There have been 47 typhoons that have hit southern Vietnam between 1954 and 1991. The highest monthly frequency of typhoons is documented in the flood season (Imamura and To, 1997). The most destructive typhoon in recent years was Typhoon Linda in November 1997, which introduced strong erosion along the eastern coast of the Mekong Delta. Modeled results show that the combination of the flood and Typhoon Linda can introduce up to 0.6–0.8 m of inundation along the MRD estuaries as far as 70 km inland (Le et al., 2007).

### 2.2. Southeast Asian monsoon

Controlled by the Southeast Asian monsoon, both the hydrological regime and estuarine/nearshore hydrodynamic systems of the Mekong River exhibit two contrasting scenarios annually. The first scenario occurs when the southwest monsoon brings more than 80% of the annual precipitation during the rainy season, which is usually between May and October (Debenay and Luan, 2006). Water discharge at Phnom Penh, Cambodia, reaches a maximum in October and a minimum in May (Gagliano and McIntire, 1968; Milliman and Meade, 1983; Wolanski et al., 1998). The majority of suspended sediment is exported to coastal waters (Wolanski et al., 1996). The second scenario occurs during the dry season when both precipitation and water discharge are limited. Tidal asymmetry, together with limited fresh water supply, generates a salt water intrusion that can reach 50 km upstream, pumping the sediment upstream (Wolanski et al., 1998).

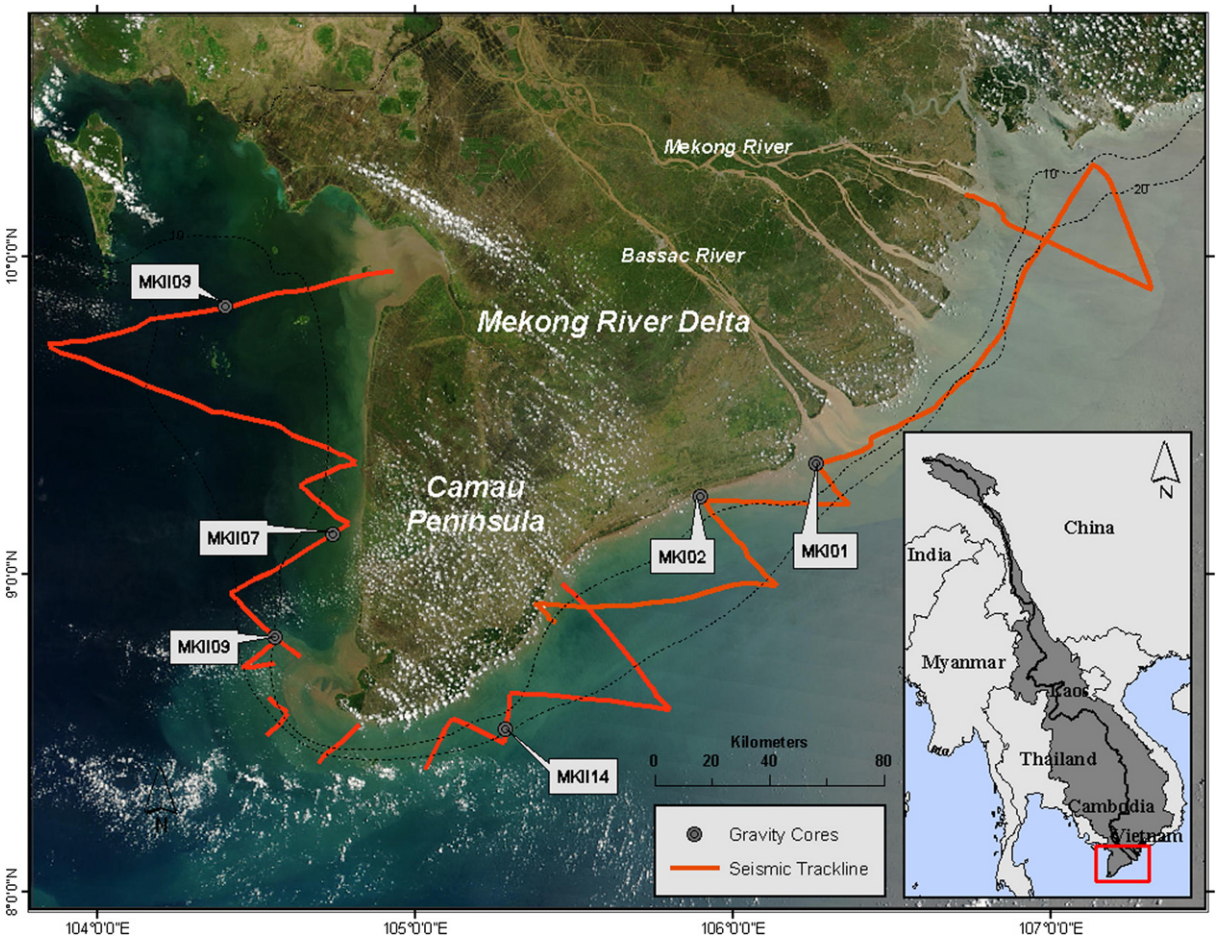


**Fig. 1.** Location map of the study area, positions of seismic tracklines and gravity cores. Satellite image courtesy of NASA (MODIS, August 2002).

The hydrodynamics of the southern Vietnam shelf are strongly influenced by the Southeast Asian monsoon (Hu et al., 2000). Modeled results in the Mekong River mouth reveal that currents can reach 0.55 m/s with directions shifting between NE in winter and SW in summer (Kubicki, 2008). For the nearshore area of the MRD, a general consensus is that waves and currents generated by the strong NE monsoon during the dry season dominates the net alongshore sediment transport (Gagliano and McIntire, 1968; Nguyen et al., 2000). Previously deposited Mekong River sediments are resuspended from the seabed, with fine particles transported and deposited several hundred kilometers away to the southwest coast of the Camau Peninsula (Nguyen et al., 2000; Liu et al., 2009).

### 2.3. Delta plain development

Sea-level research on the Sunda Shelf reveals that sea-level was about −120 m around 19,000 to 20,000 cal yr BP (Hanebuth et al., 2009). For the MRD, a sea-level curve for the last 15,000 cal yr was developed, based on inland boreholes (Ta et al., 2002a). Both the sea-level curve of the Sunda Shelf and that of the MRD show a rapid sea-level rise since the last glacial episode. After reaching its maximum height around 5500 cal yr BP, sea-level has been slightly falling until recently.

Sedimentological and stratigraphic analyses of boreholes on the lower delta plain indicate that postglacial sea-level rise and transgression have caused the infilling of an incised paleo-valley (Ta et al., 2005). The upcore sequence in deposits ranges from marsh and estuarine sediments to open-bay deposits to pro-delta and delta-front sediments, capped by subtidal and intertidal deposits and beach ridges (Ta et al., 2005). $^{14}C$ measurements indicate that the initial development of the MRD was around 8000 cal yr BP after the mid-Holocene sea-level highstand (Tamura et al., 2009). Since then, the subaerial part of the MRD has continuously prograded more than 250 km from Cambodia border toward the South China Sea (Nguyen et al., 2000). Over the past 3000 cal yr, the modern delta plain and the sediment below (including paleo-subaqueous deltaic deposits) have accumulated about $360\times10^9$ m$^3$ of sediment, which is equal to 144 million tons of sediment per year (Ta et al., 2002a). At the same time, sequence stratigraphic analyses indicate that the last 3000 cal yr were characterized by delta progradation changing from tidal influenced to increasingly wave influenced southward sediment dispersal. During this period the rate of delta progradation decreased, and the facies of the delta front steepened (Ta et al., 2002a).

## 3. Data and methods

Two research cruises were conducted in April 2006 and March 2007 by the Sea-level Change and Ocean Margin Evolution Laboratory at North Carolina State University (NCSU). The research is a joint study with the Institute of Geography, Vietnam National Center for Natural Science and Technology. Approximately 1150 km of high-resolution seismic profiles were obtained using an EdgeTech 0512i Chirp Sonar Sub-bottom Profiler (frequency range: 0.5–12 k) together with a number of gravity cores (for seismic tracklines and core positions see Fig. 1; for details of gravity cores in this study see Table 1).

In the laboratory at NCSU, seismic and navigation data were processed using EdgeTech Discover Sub-bottom software (Version 3.27). Grain size analysis (4–5 samples per core with 10 cm intervals) was done using a LS 13 320 Laser Diffraction Particle Size Analyzer (Beckman Coulter©, size range 0.4 μm–2000 μm, Table 1). $^{210}Pb$ activities were determined following a procedure similar to that of DeMaster et al. (1994). Calculated $^{210}Pb$ activities were normalized to the sample's mud contents (grain size less than 63 μm).

The majority of the sediment cores recovered in this study consisted of brown-colored mud with few foraminifera. Foram shell samples were only found in cores located on the northwest shore of the Camau Peninsula. Because no continuous distribution of a particular species occurred down core with sufficient abundance, $^{14}C$ chronologies and organic carbon ($C_{org}$) stable isotope ratios ($\delta^{13}C$) were established on the $C_{org}$ content of the bulk-sediment. The $C_{org}$ samples were prepared following a method similar to that of Leithold et al. (2006). $CO_2$ produced from the combustion of the organic matter was analyzed for carbon isotopic ratios using a Delta V IRMS with a standard dual inlet. $CO_2$ from the C/N elemental analyzer (FLASH 1112 Series) was collected cryogenically and sent to the WHOI National Ocean Sciences AMS facility, where it was converted to graphite and analyzed for its $^{14}C$ content using accelerator mass spectrometry.

## 4. Results

High resolution seismic records (Figs. 3, 4, 6–8) revealed the stratigraphic structure of a subaqueous delta system (<30 m water depth), surrounding the modern MRD. Generally, seismic profiles showed a prominent subsurface reflector, overlain by a thick clinoform that thinned offshore. Relatively high-gradient foreset strata occurred seaward of the Mekong River mouth and near Cape Camau. The boundary of the subaqueous delta front is shown in Fig. 2. Based on differences in the nature of the clinoform and associated sediment, this subaqueous delta was divided into four zones as described below (Table 2).

Between 1997 and 2000, a number of borehole cores were successively retrieved on the MRD plain. A schematic delta evolution model was developed covering sedimentation facies since the last sea-level low stand (Nguyen et al., 2000, 2005; Ta et al., 2001a,b, 2002a,b, 2005)(see core positions in Fig. 2). We refer to these boreholes to correlate the facies architecture within the subaqueous delta.

Six cores were analyzed for their $^{210}Pb$ activity. Supported levels were determined by averaging the total $^{210}Pb$ activities from the bottom of selected cores (primarily MKII14 and MKII07; the latter core had a raw $^{14}C$ age of 3120 yr in its deepest samples). Based on the counting statistics, the error in total $^{210}Pb$ activities is 3%–5%. This error range is negligible to that of the support level, which is 0.3 dpm/g mud as a most realistic assumption. A supported level of $1.44\pm0.3$ dpm/g mud was

**Table 1**
Details of gravity cores used in this study.

| Core no. | Longitude (°) E | Latitude (°) N | Water depth (m) | Core length (cm) | Vertically averaged grain size (μm)* | % of volume | | |
|---|---|---|---|---|---|---|---|---|
| | | | | | | Clay | Silt | Sand |
| MKI01 | 106.265 | 9.347 | 4.5 | 15 | – | – | – | – |
| MKI02 | 105.900 | 9.243 | 5.0 | 27 | – | – | – | – |
| MKII03 | 104.408 | 9.841 | 15.6 | 57 | 36.84 | 14.54 | 61.99 | 23.47 |
| MKII07 | 104.743 | 9.125 | 10.0 | 49 | 14.79 | 31.11 | 66.03 | 2.86 |
| MKII09 | 104.561 | 8.801 | 10.0 | 101 | 11.87 | 33.81 | 64.81 | 1.39 |
| MKII14 | 105.288 | 8.512 | 16.0 | 50 | 40.14 | 24.03 | 48.26 | 27.71 |

*Averaged over 10 cm interval.

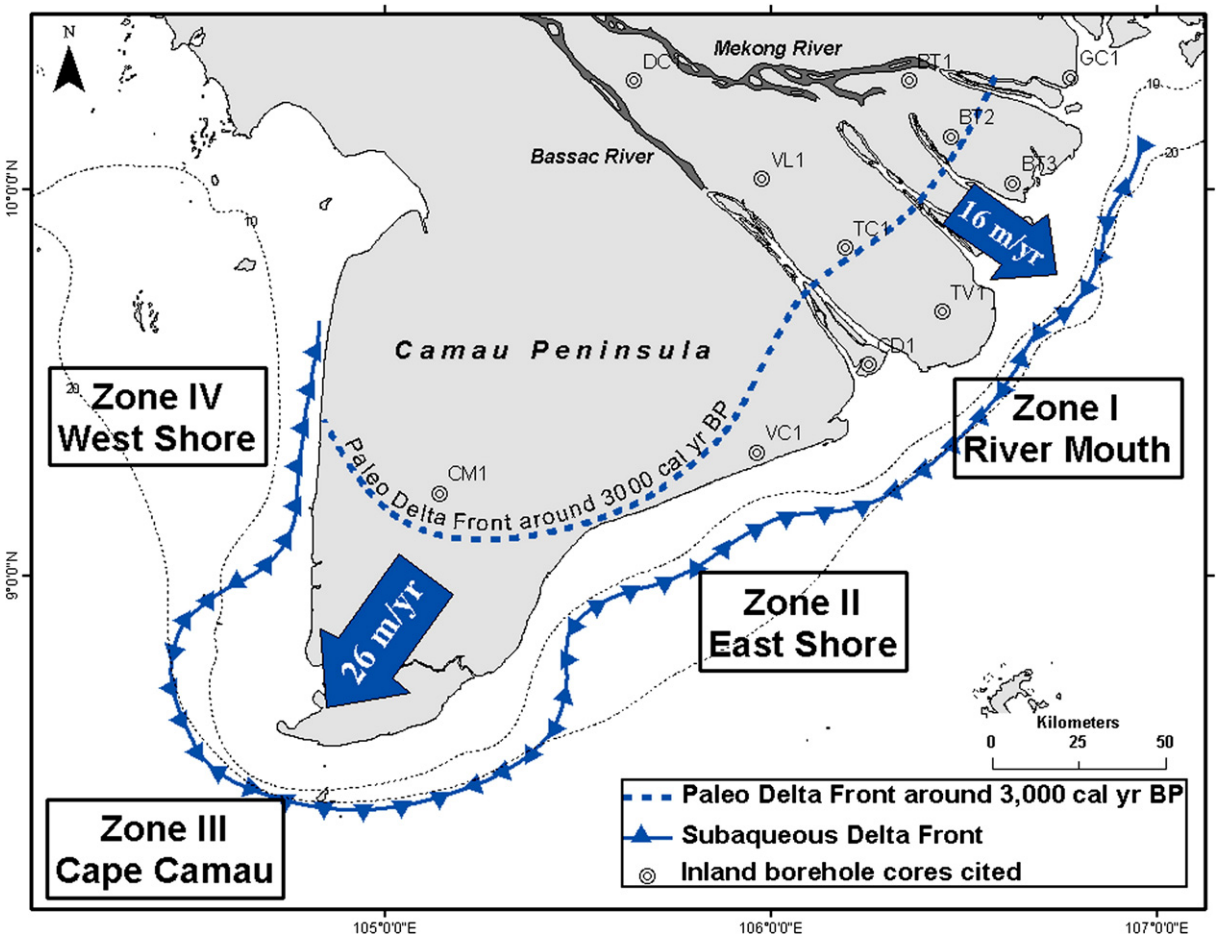


**Fig. 2.** The zonation of the Mekong River Delta (Zone I. Mekong River mouth, Zone II. East shore of Camau Peninsula, Zone III. Cape Camau, and Zone IV. West shore of Camau Peninsula). The blue dashed line is the paleo delta front around 3000 yr BP after Nguyen et al. (2000) and Ta et al. (2002b).

used for cores located on the east shore (cores MKI01, MKI02, and MKII14) and 1.09 ± 0.3 dpm/g mud for cores located on the west shore (cores MKII03, MKII07, and MKII09) to calculate excess $^{210}$Pb activities in the seabed.

The $^{14}$C data reported in this study for the Mekong shelf are given as "raw" $^{14}$C ages, i.e., they have been normalized to a common $\delta^{13}$C value, but not corrected for a reservoir age or atmospheric $^{14}$C/$^{12}$C variations. These relative ages (reported in $^{14}$C yr) were used to assess the nature of sedimentation at a given coring site and were not used for age correlation with the $^{14}$C data from the boreholes (which were reported in units of $^{14}$C yr BP).

### 4.1. Zone I. Mekong River mouth

Zone I is located seaward of the Mekong River mouth (Fig. 2). Water depth increases sharply seaward of the river mouth. Portions of two seismic profiles recovered from this area, i.e. Line 2006-1 (cross shore) and Line 2006-3 (parallel to shoreline), are shown in Figs. 3 and 4.

Line 2006-1 (Fig. 3) shows a high-gradient foreset bed compared to the rest of the clinoform structures in the east shore and west shore of the Camau Peninsula. It has a smooth outline and the gradient of the foreset strata is approximately 2.5:1000. The delta front has a very limited bottomset bed and a foreset bed up to 15 m thick, which consists of a succession of sub-parallel strata. The foreset strata are correlated to the delta front facies in Cores BT2 and BT3, which was described as a 7 to 10 m intercalated greenish gray silt, sandy silt, and fine sand layer (see cross section BT2–BT3 in Fig. 3a and c). Underlying the foreset strata is a ~5 m thick transparent layer that can be correlated to the pro-delta/shelf mud facies of Core BT2. The strata end at ~20 m depth with an uneven strong reflection, which reflects the sharply increased sand content documented in Core BT3 at the same depth. Although this sand layer in BT3 was initially regarded as a transgressive sand layer, its $^{14}$C age is between 4000 and 4200 cal yr BP, indicating that it was formed by a regressive erosion episode instead of a transgressive one (Ta et al., 2002a).

Line 2006-3 (parallel to shoreline) reveals an incised valley fill (Fig. 4b). This seismic track is located ~20 km seaward of the modern

**Table 2**
Clinoform and sediment characters along the coastal area in MRD.

| Zone | Gradient | Seismic profile reflectivity | Excess $^{210}$Pb profile | Source of organic matter | Grain size |
|---|---|---|---|---|---|
| I | ~2.5:1000 | Strong | Near surface excess only | – | Sand-clay-silt mixing |
| II | ~0.8:1000 | Strong | Uniform limited to no excess activity | Mixture of terrestrial/marine | Sand-clay-silt mixing |
| III | ~5.0:1000 | Moderate | Uniform activity with limited excess activity | Mixture of terrestrial/marine | Clayey silt |
| IV | ~1.0:1000 | Weak | Some decrease in excess activity | Mostly marine | Clayey silt |

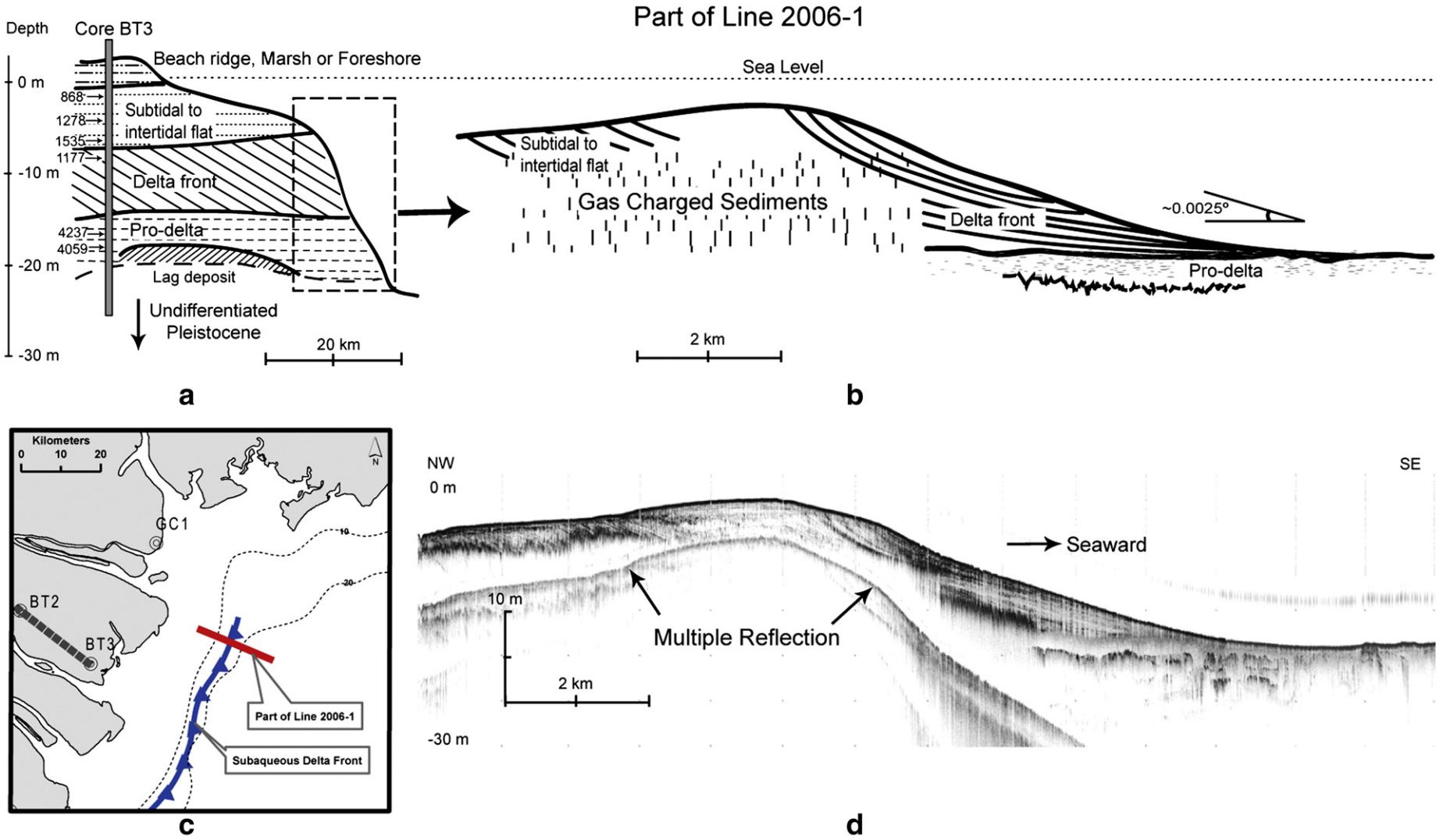


**Fig. 3.** Seismic trackline 2006-1 seaward of the Mekong River mouth. a. Sedimentation facies based on inland boreholes by Ta et al. (2005); b. schematic facies architecture; c. position maps of inland boreholes, cross section and seismic trackline; d. seismic "Chirp" profile.

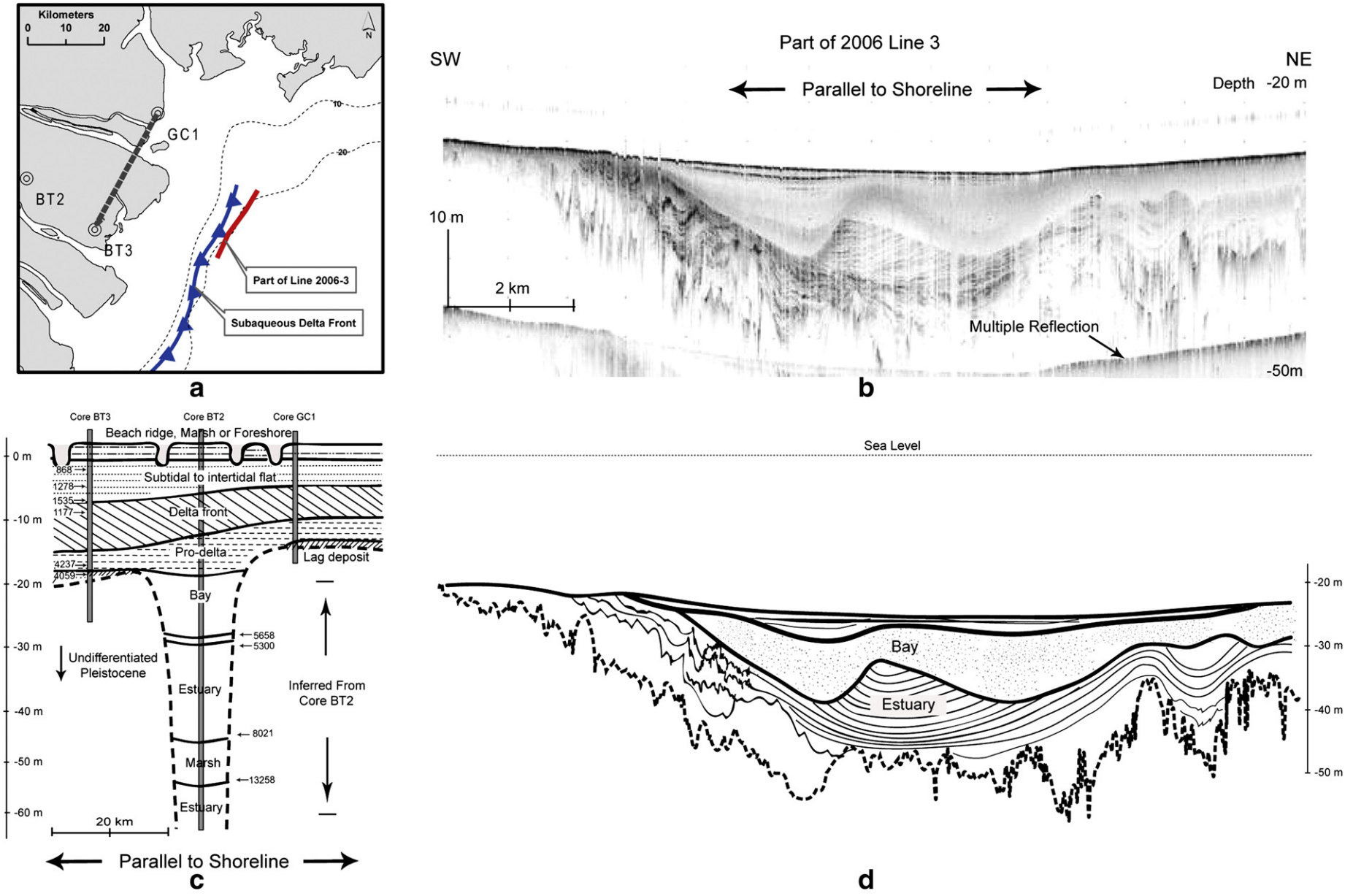


**Fig. 4.** A filled incised valley seaward of the Mekong River mouth. a. Position maps of inland boreholes, cross section and seismic trackline; b. seismic "Chirp" profile; c. sedimentation facies based on inland boreholes by Ta et al. (2002b); d. schematic facies architecture.

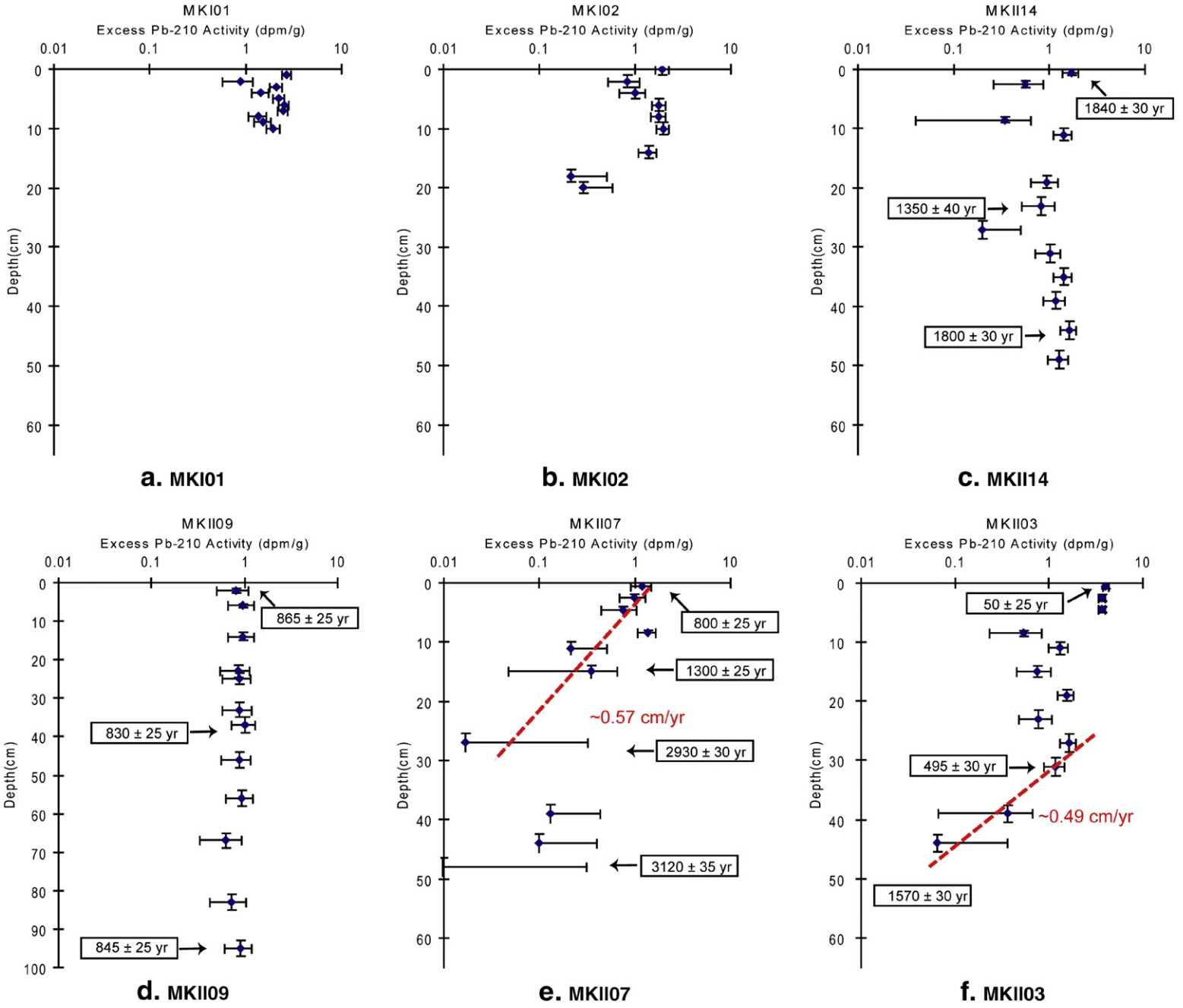


**Fig. 5.** Excess $^{210}$Pb profiles of sediment cores from Zone I (a and b), Zone II (c), Zone III (d), and Zone IV (e and f).

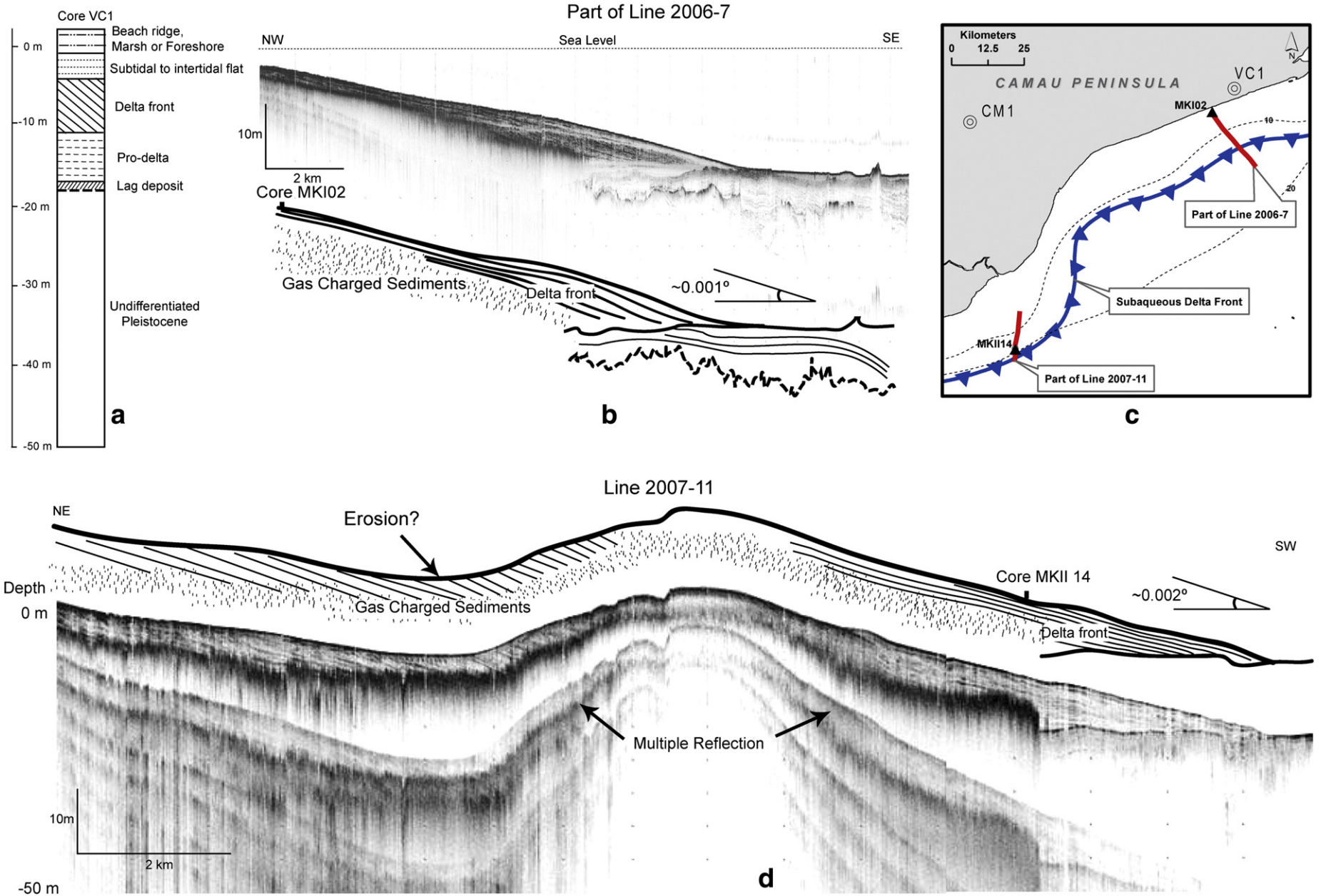


**Fig. 6.** Seismic profiles from Zone II: 2006-7 and 2007-11. a. Sedimentation facies based on borehole VC1, by Ta et al. (2005); b. seismic "Chirp" profile with schematic facies architecture of line 2006-7; c. position maps of inland boreholes, cross section and seismic trackline; d. seismic "Chirp" profile and schematic facies architecture of line 2007-11.

river mouth (~20 m water depth). Its facies can be well correlated to the lower part of Core BT2 (Fig. 4a), which shows an incised valley fill sequence recovered on the MRD plain (Ta et al., 2002a, 2005). On the top of the profile there is ~2 m thick weak lamination. Underneath, there is a 12–20 m thick weak reflection with a "ω" shape bottom deeply cutting into the underlying sediments. This weak reflection is correlated to the bay facies, which consists of homogenous greenish-grey mud with little grain size variation (Ta et al., 2002a). The deep cut was probably formed by a landward migrating tidal inlet during high sea-level stand, similar to the one documented outside the Gironde Estuary in France (Allen and Posamentier, 1993).

Beneath the homogeneous weak reflection unit there is a 15–25 m thick layer of subparallel strata, coinciding with the estuarine facies in Core BT2 between 37 and 55 m depth. This estuarine facies is characterized by intercalated yellowish-grey coarse sand and greenish-grey silty sand (Ta et al., 2001a). Further down, the seismic profile shows discontinuous strata, which is correlated to the marsh facies in BT2 dated at 13,258 ± 115 cal yr BP. The incised valley fill sequence is terminated by an uneven strong reflector at a depth of 60 m.

A shallow gravity core, MKI01 (position see Fig. 1), was recovered seaward of the Bassac River mouth (~4.5 m water depth). There is an excess $^{210}$Pb-riched layer in the top 10 cm, which could be an ephemeral deposit or a seasonal surface layer (Fig. 5a). A clear drop in excess $^{210}$Pb activity was observed at 11 cm depth. Another core, MKI02, located 40 km southwest along the coast, also showed a similar drop in excess $^{210}$Pb activity at a similar depth (Fig. 5b). These sharp drops of $^{210}$Pb activity may be caused by event sedimentation such as flooding. Because of their short length (<40 cm), cores in this area were not analyzed for $^{14}$C or $\delta^{13}$C activity.

### 4.2. Zone II. East shore of the Camau Peninsula

Zone II is along the east shore of the Camau Peninsula (Fig. 2), where the coastline has been under serious erosion at a rate of 1.1 km$^2$/yr since 1885 (Saito, 2000). Clinoforms in this area are characterized by low-gradient foreset strata.

Fig. 6 shows parts of two cross-shore seismic profiles, i.e. Line 2006-7 (Fig. 6b) and Line 2007-11 (Fig. 6d). Both have a low-gradient foreset (<5:1000). Line 2006-7 has up to 20 m thick foreset beds with sub-parallel strata, which are correlated to the delta front facies in Core VC1, 10 km northwest, at a depth between 5 m and 11 m. Underlying the foreset beds is an ~8 m thick transparent layer. An uneven surface with strong reflectivity was observed at a depth of ~25 m. Line 2007-11 has up to 8 m thick foreset beds directly overlying a strong reflector at ~20 m depth. There is a remarkable concave feature in the middle of the topset (Fig. 6d), which may be the result of coastal erosion as described above.

Core MKII14 (14.5 m water depth) was retrieved from the seaward limit of the clinoform shown on Line 2007-11 (Fig. 6d). The sediments are made up of a mixture of clay, silt, and sand dominated by silt (48.26%, Table 1). Grain size shows little variation throughout the 50-cm-long core. MKII14 shows minimal excess $^{210}$Pb activity (Fig. 5c). The excess $^{210}$Pb activity profile suggests that the sediments may have deposited at a high accumulation rate. The radiocarbon data give "raw" $^{14}$C ages on the order of 1310–1870 yr (Table 3, Fig. 5c). $\delta^{13}$C values of these samples vary between −23.2 and −23.6‰. These $^{13}$C data suggest a mixed terrestrial/marine source for the bulk $C_{org}$. The thousand year old bulk $C_{org}$ $^{14}$C ages are consistent with the preponderance of the organic matter coming from the accumulation of old terrestrial soil organic matter from land.

### 4.3. Zone III. Cape Camau

In Zone III the strata exhibited a series of high-gradient foreset layers between 11 m and 25 m water depth. From the tip of Cape Camau to the northwest, reflectivity of the clinoforms is much weaker than in Zones I and II. Sediments varied from a mixed sand-silt-clay to a clayey silt (Table 1).

Line 2007-15 (Fig. 7a) showed relative steep foreset strata (~5:1000). The topset, overlying intensive gas-charged sediment, was flat and continuous to the shore. A strong reflector was located at ~30 m depth. Compared with Line 2007-15, the foreset strata shown by Line 2007-6 were weak in reflectivity and low in gradient (~1:1000, Fig. 7d). Both profiles show gas-charged sediment underlying the topset.

Core MKII09 (10.0 m water depth) was located on the foreset of the clinoform on Line 2007-6 (Fig. 7d). This 100-cm-long gravity core primarily was composed of fluid mud. Grain size shows little variation throughout the core. All three bulk sediment samples from the top (2 cm), middle (40 cm), bottom (100 cm) have a $^{14}$C age around 850 yr (Table 3, Fig. 5d). The $\delta^{13}$ C measurements indicate that the $C_{org}$ at this site is a mixture of terrestrial/marine origin (−24.1 to −24. 4‰, Table 3). The $^{210}$Pb activity profile from Core MKII09 shows no minimal excess activity throughout the core. The reason for the lower bulk organic matter $^{14}$C ages in core MKII09 in Zone III (ages ~850 yr) relative to the core MKII14 in Zone II (ages 1310–1870 yr) is not know because the stable carbon isotopic data at core MKII09 indicated a more terrestrial (or old) $C_{org}$ source ($\delta^{13}$C ~ −24.2‰) compared to MKII14 ($\delta^{13}$C ~ −23.2 to −23.6‰).

**Table 3**
AMS $^{14}$C ages of sedimentary bulk organic matter.

| Core No. | Water depth (m) | Sample depth (cm) | $^{14}$C age (yr) | $\delta^{13}$C (per mil) |
|---|---|---|---|---|
| MKII-3 | 15.6 | 0–1 | 50 ± 25 | −21.2 |
| | | 30–32 | 495 ± 30 | −20.6 |
| | | 55–57 | 1570 ± 30 | −20.8 |
| MKII-7 | 10.0 | 0–1 | 800 ± 25 | −24.3 |
| | | 14–16 | 1300 ± 30 | −22.7 |
| | | 30–32 | 2930 ± 30 | −23.8 |
| | | 46–48 | 3120 ± 35 | −24.2 |
| MKII-9 | 10.0 | 0–4 | 865 ± 25 | −24.2 |
| | | 39–41 | 830 ± 25 | −24.1 |
| | | 99–101 | 845 ± 25 | −24.4 |
| MKII-14 | 16.0 | 0–1 | 1840 ± 30 | −23.3 |
| | | 18–20 | 1350 ± 40 | −23.6 |
| | | 48–50 | 1800 ± 30 | −23.2 |

*The $^{14}$C data are "raw" ages that have been normalized to a constant $\delta^{13}$C value, but have not been corrected for a reservoir age or atmospheric $^{14}$C/$^{12}$C variations.

### 4.4. Zone IV. West shore of the Camau Peninsula

As part of the Gulf of Thailand, the west shore of the Camau Peninsula is dominated by an irregular diurnal tide with a range of 0.8–1.0 m (Le et al., 2007). This part of the peninsula experienced rapid progradation at a rate of 1.2 km$^2$/yr between 1885 and 1985 (Saito, 2000). The lower part of the Camau Peninsula (roughly from Core CM1 to the south, Fig. 2) was not formed until 3000 cal yr BP (Nguyen et al., 2000). Here we refer to Borehole CM1 (Nguyen et al., 2005) for facies correlation.

Clinoforms in this zone generally have low gradients and low reflectivity. Two cross shore profiles, Line 2007-1 and Line 2007-5, are shown in Fig. 8. The clinoform in Line 2007-5 exhibited a very gentle foreset with a gradient of 0.6:1000. The majority of the foreset strata are transparent with weak laminae (Fig. 8a). Only a very limited delta front with strong reflectivity developed and ended at 10 m water depth, leaving the majority of the shelf/pre-delta facies uncovered. A strong reflection was observed at ~20 m depth. The subaqueous delta front ended between the east end of Line 2007-2 and Line 2007-1. No distinct deltaic facies was observed on Line 2007-1, which exhibited a homogenous light reflector overlying on an uneven paleo-surface with strong reflectivity (Fig. 8d).

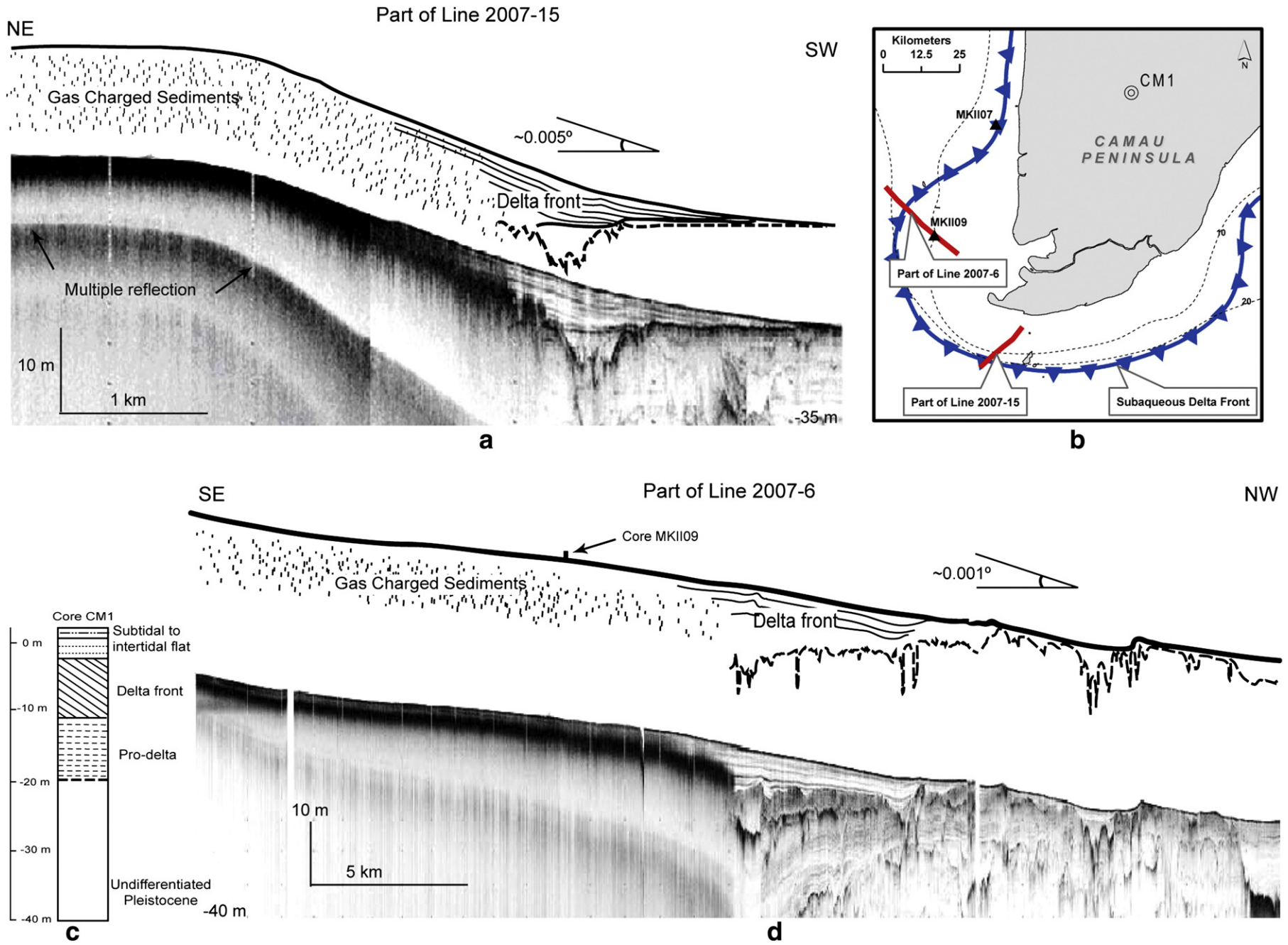


**Fig. 7.** Seismic profiles in Zone III: 2006-7 and 2007-11. a. Seismic "Chirp" profile and schematic facies architecture of line 2007-15; b. position maps of inland boreholes and seismic tracklines; c. sedimentation facies based on borehole CM1, after Nguyen et al. (2005); d. seismic "Chirp" profile and schematic facies architecture for line 2007-6.

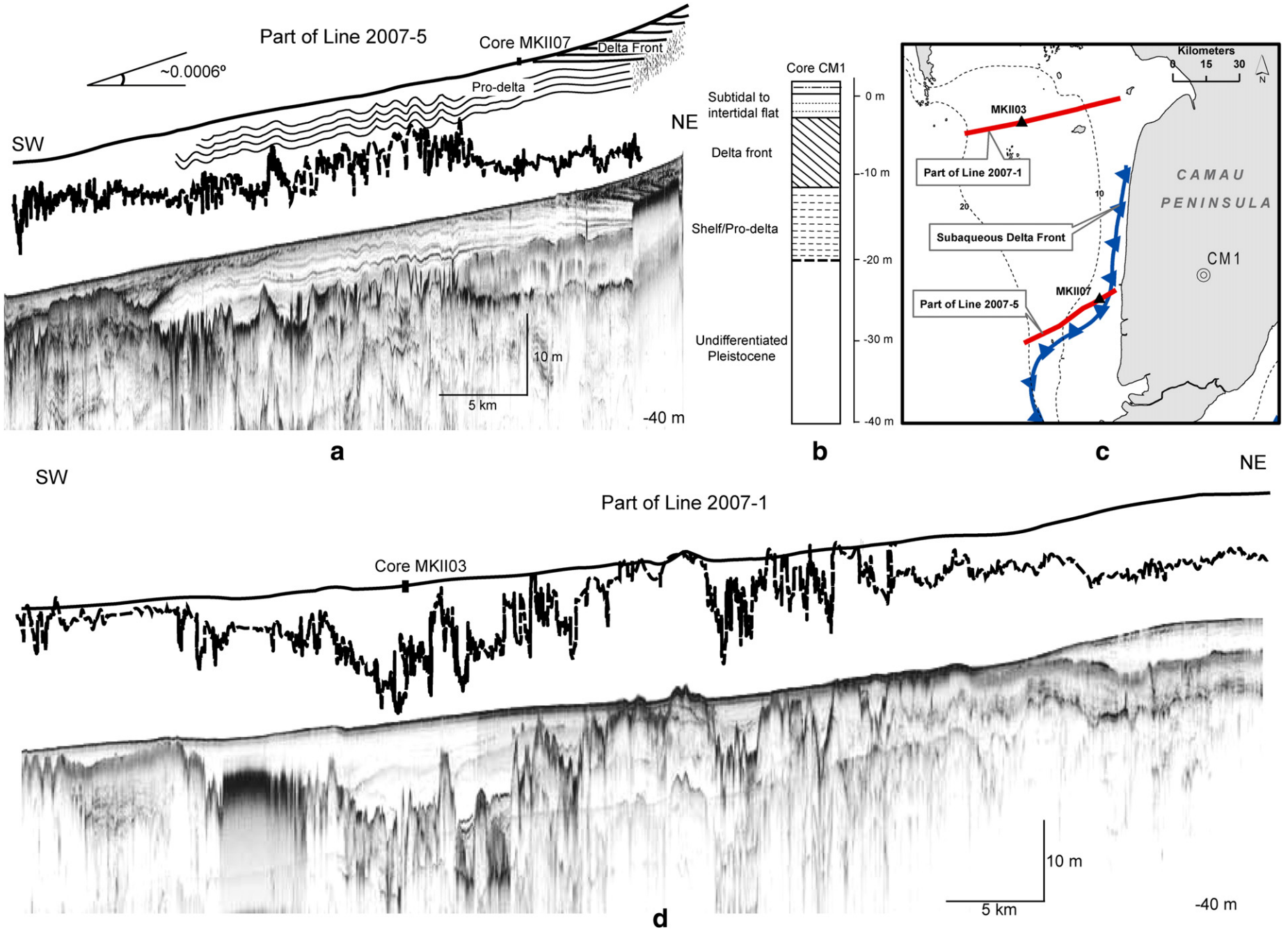


**Fig. 8.** Seismic profile from Zone IV: 2007-1 and 2007-5. a. Seismic "Chirp" profile and schematic facies architecture of line 2007-5; b. sedimentation facies based on borehole CM1 by Nguyen et al. (2005); c. position maps of inland boreholes and seismic tracklines; d. seismic "Chirp" profile and schematic facies architecture for line 2007-1.

Core MKII07 (10 m water depth) was collected from the seaward limit of the delta front (on Line 2007-5, see Fig. 8a). It mainly consists of clayey silt with little vertical variation. An oyster shell sample was observed at 12 cm depth. Calculated accumulation rate for the upper 30 cm of this core is ~0.57 cm/yr (Fig. 5e). $^{14}C$ measurements of the $C_{org}$ from the top (1 cm), upper middle (15 cm), lower middle (31 cm), and bottom (47 cm) yield ages of 800 ± 25, 1300 ± 25, 2930 ± 30, and 3120 ± 35 yr (Table 3). $\delta^{13}C$ values of these four samples indicate that the $C_{org}$ is from a mixed terrestrial/marine source (−23.26 to −24.16 ‰, comparable with that of Cores MKII09 and MKII14). If the $^{14}C$ age of the organic matter at the surface seabed has remained constant over time, the radiocarbon data suggest an accumulation rate as low as 0.02 cm/yr for this core.

Although the majority of the cores collected in this study are made up of brown-colored muddy sediments with high porosity, core MKII03 along Line 2007-1 (6 m water depth, position see Fig. 8c) was made up of greenish silt. $^{210}Pb$ profiles of cores MKII03, located on the weak reflector on Line 2007-1 (Fig. 8d), are shown in Fig. 5f. Excess $^{210}Pb$ activity in the top 30 cm of MKII03 shows excess activities in the upper 5 cm, overlying a zone of uniform activity with minimal excess activity, depending on the supported $^{210}Pb$ activity chosen. Below the zone of uniform activity the total $^{210}Pb$ activity decreases, but this may be due to a change in sediment type (e.g., grain size, or organic matter content). Calculated accumulation rate below the zone of uniform activity is ~0.49 cm/yr (Fig. 5f).

Shell samples were found at 12 cm, 45 cm and 49 cm depth in this core. $\delta^{13}C$ values of three samples from the top (1 cm), middle (31 cm) and bottom (54 cm) of this core vary between ~−20.65 and ~21.23‰, indicating a greater contribution of marine plankton to the bulk organic matter content of this core as compared to the other cores examined in this study. Bulk $C_{org}$ $^{14}C$ measurements from the surface (1 cm), middle (31 cm), and bottom (54 cm) of this core yielded ages of 50 ± 25, 495 ± 30, and 1570 ± 30 yr, respectively. The younger $^{14}C$ ages are consistent with the greater relative abundance of marine planktonic organic matter at this site (as indicated by the $\delta^{13}C$ data). If the $^{14}C$ age of the bulk organic matter at the sediment–water interface is assumed to remain constant over time, the radiocarbon data indicate an accumulation rate of ~0.03 cm/yr.

## 5. Discussion

### 5.1. Asymmetric delta evolution

Because of the large amount of fluvial sediment input and a decreasing sea-level, the MRD has prograded 250 km from the Cambodia border to the South China Sea in the last 6000 yr (Nguyen et al., 2000). However, the progradation process is not constant throughout the late Holocene. After the delta body refilled the former bight, the delta edge began to be exposed to longshore currents. A phase shift from “tidal dominated” to “wave and tidal dominated” around 3000 cal yr BP has been reported, based on facies changes in inland boreholes (Ta et al., 2002a). In contrast, to the “tidal dominated” regime, a “wave and tidal dominated” MRD is characterized by a large subaerial delta plain, longshore sediment dispersal, and steep delta-front topography in the proximal delta (Ta et al., 2005). Although the subaqueous delta front has had a high progradation rate over the past 3000 yr, on a smaller time scale its development is a non-linear process with cycles of deposition and erosion. In Zone II where both tide and wave energy is strong, the MRD is suffering serious erosion (Saito, 2000). The seismic profile also shows scour/erosion of the clinoform structure (see Line 2007-11 in Fig. 6d).

An ‘asymmetric delta model’ was first proposed by Bhattacharya and Giosan (2003) to describe the morphological and facies difference between the updrift and downdrift of a wave-influenced deltaic system. For the first time, high resolution seismic profiles reveal a subaqueous delta surrounding the MRD with a morphological asymmetry. The highest delta progradation rate (~26 m/yr, Fig. 2) is found around Cape Camau, ~200 km downstream from the river mouth. This, together with the huge downdrift area of the MRD, indicates the importance of longshore sediment transport in MRD's evolution over the past 3000 yr.

### 5.2. Longshore sediment transport

The Lower Mekong region is controlled by the Southeast Asian monsoon and shows two contrasting scenarios annually. During the wet season (May to November), large amounts of sediment are transported toward the river mouth and temporarily deposit there. During the following dry season (December to April), a large part of previously deposited sediment will be resuspended from the seabed by the tidal currents and surface waves. The resuspended sediments are then either bumped upstream (Wolanski et al., 1998), or transported southwestward by coastal current strengthened by strong NE monsoon (Gagliano and McIntire, 1968; Nguyen et al., 2000; Liu et al., 2009). Changes in tidal amplitude and location of the salinity front contribute to the formation of the inter-layered sands and muds (Kineke et al., 1996). These processes may explain the limited subaqueous delta front seaward of the river month with a succession of sub-parallel strata (Zone I). A similar remobilization of temporary deposits during the energetic periods has also been reported on the Amazon shelf (Allison et al., 1995).

A calculation by Geyer et al. (2004) indicates that a surface river plume can only transport flocculated sediments for 5 km while a bottom resuspension can maintain sediment in the water at large distances from the river mouth. Both surface wave and tidal currents contribute to the resuspension of previously deposited Mekong sediments, which are then transported southwestward by coastal currents along the eastern shore of the Camau Peninsula (Zone II).

Cape Camau is located at the intersection of two different tidal systems: to the east, a regular semidiurnal tide with 3.5 m tidal range for the South China Sea, and to the west, an irregular diurnal micro-tide with 0.8–1.0 m tidal range for the Gulf of Thailand. Due to reduced tidal energy, a large amount of longshore transported sediment settles out and accumulates, forming a series of high-gradient clinoforms with high-gradient foresets (Zone III, Fig. 7). Only fine sediment can pass the tip of the cape and reach the western shore of the peninsula, which, combined with the micro-tide from the Gulf of Thailand, explains the low-gradient clinoform structures in Zone IV (low reflectivity and blurred laminae, Fig. 8a).

Instead of a dominant marine source, organic matter in the sediments of the Mekong continental shelf has two potential sources, which are in situ primary productivity and terrestrial organic matter from fluvial sediments. A significant part of the later source may be from ‘old’ terrestrial soils. For the Mekong subaqueous delta, the average fluvial sediment input may be as high as 160 million tons per year, making the source of the $C_{org}$ in the coastal area inevitably a mixed one. $^{14}C$ measurements in this study yield few young ages for bulk organic matter (except at site MKII03) on the subaqueous delta, indicating a contribution of ‘old’ organic material supplied by fluvial sediments or resuspension of previously deposited sediments. The $\delta^{13}C$ values confirm a mixed terrestrial/marine source (Cores MKII14, MKII09, and MKII07, Table 3).

Although the $^{210}Pb$ profiles on the subaqueous delta show limited excess activity, a lower limit on the sediment accumulation rate can be estimated from the $^{14}C$ data, which suggests high rates in cores MKII14 and MKII09 (rates are not available because of rapid accumulation or physical mixing) located around the rapidly prograding Cape Camau and slower rates (0.02–0.03 cm/yr) in cores MKII07 and MKII03 located in the Gulf of Thailand with weak hydrodynamics. Compared with the accumulation rate revealed by inland boreholes (0.45 cm/yr for the prodelta facies and 0.29–0.42 for the delta front facies, Ta et al., 2005), accumulation rate estimated from the $^{14}C$ data of Gulf of Thailand sediments is much lower. This is

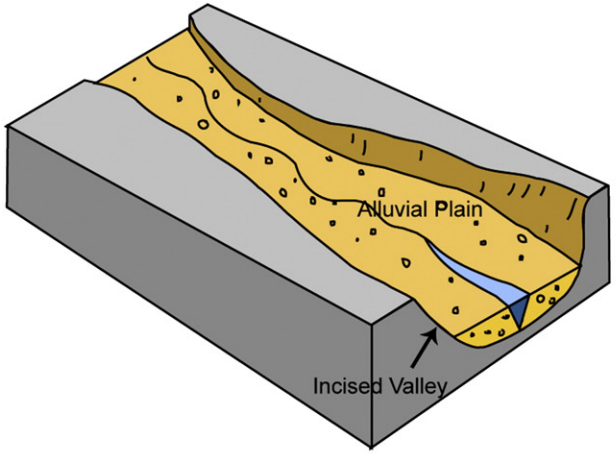


**a.** Low sea-level stand
(prior to LGM)

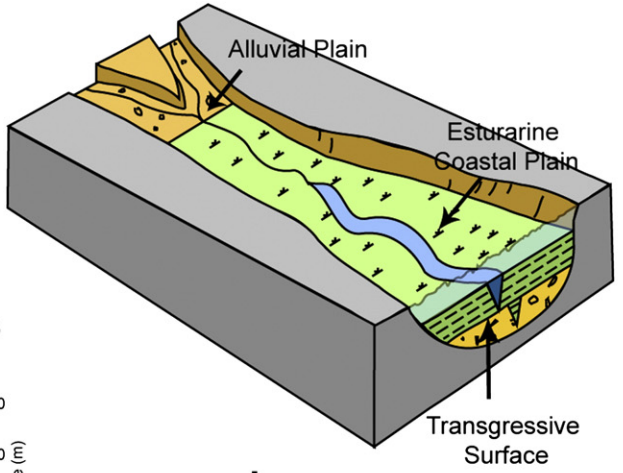


**b.** Transgression
(after 19,000 ~ 20,000 cal yr BP)

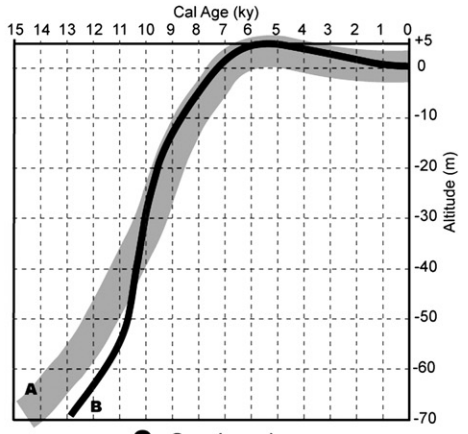


**e.** Sea Level

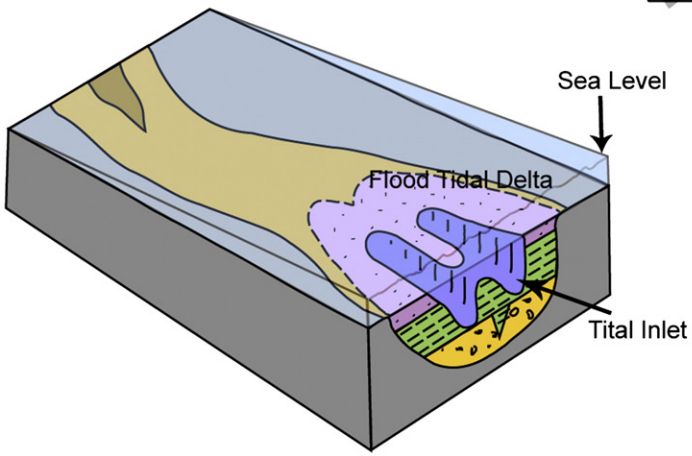


**c.** High sea-level stand
(~ 5,500 cal yr BP)

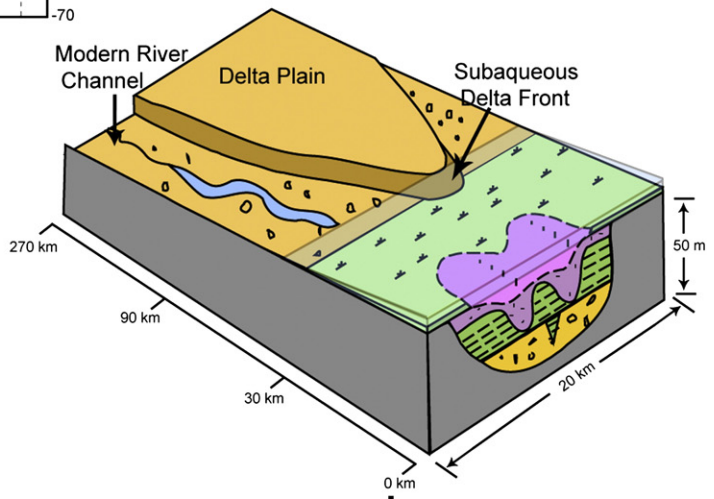


**d.** Modern

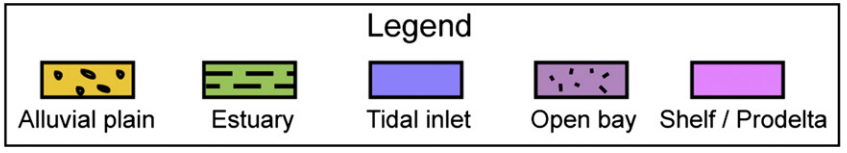

reasonable as those inland boreholes were retrieved from paleo-river mouths that have a high progradation rate (16 m/yr, this study).

### 5.3. Late Holocene sediment budget

Previous studies show that the paleo-delta front break was around the location of Core BT2, Core TC1 and the center of Camau Peninsula around 3000 cal yr BP. The progradation rate of Mekong delta was 20–30 m/yr in the last 2500 yr (Nguyen et al., 2000; Saito, 2000; Ta et al., 2002b, Fig. 2). However, due to a lack of subaqueous data, the position of the modern delta front break was based on bathymetric estimation. Seismic profiles in this study successfully delimit the subaqueous delta. The progradation rate of the MRD over the last 3000 yr is updated to a value of ~16 m/yr around river mouth and ~26 m/yr around the tip of Camau Peninsula in the south.

Previous sediment volume estimation in Ta et al. (2002b) used an averaged deltaic sediment thickness of $20 \pm 5$ m for the study area. Here this value is adjusted to $18 \pm 5$ m because the thickness of most of the subaqueous deltaic sediment shown in the seismic profiles is between 10 to 20 m. Then there were 17,700 $km^2$ (area between paleo and modern delta front) × ($18 \pm 5$ m, averaged sediment thickness) × ($1.2 \pm 0.1$ $g/cm^3$, averaged dry bulk density) = $382 \pm 88$ billion tons of sediment trapped within the subaerial and subaqueous part of the MRD over the past 3000 yr.

The sediment flux of the Mekong River has not changed greatly during the last 3000 yr (Ta et al., 2002b). If we further assume the annual 160 million tons of sediment discharge is constant, then every year approximately $80 \pm 18\%$ [$(382 \pm 88 \times 10^9$ tons)/3000 yr/($160 \times 10^6$ tons/yr) × 100%] of the sediment delivered by the Mekong River have taken part into the delta's progradation. This is a reasonable result because satellite images show that the sediment plume outside the river mouth can reach areas tens of kilometers seaward of the subaqueous delta front (see Fig. 1, satellite image taken in August 2002 by NASA).

Late Quaternary sediment budget estimates have already been conducted on two other large river systems along the Western Pacific, i.e. the Yangtze and Yellow Rivers. For the Yangtze and Yellow dispersal systems, distal mud wedges/subaqueous delta lobes are found in coastal areas hundreds of kilometers away from the river mouth (Liu et al., 2004; Liu et al., 2007a,b). While for the Mekong, although longshore current has been carrying away a large amount of fluvial sediment from the river mouth, the majority of these longshore transported sediments are finally trapped within the broad shallow shelf, south of the river mouth, forming the third largest delta plain in the world (Liu et al., 2009).

### 5.4. Incised Valley Fill

Another intriguing discovery in this study is the incised valley fill seaward of the Mekong River mouth shown in Fig. 4. The initial erosion stage for most incised valleys probably occurred immediately after the exposure of the shelf during low sea-level stand. Shelf-wide regressive incisions were formed on the sub-aerial exposed Sunda shelf (Hanebuth et al., 2002; Schimanski and Stattegger, 2005). As for the MRD, the 70 m long borehole BT2 successively penetrated the incised valley fill on the modern delta plain (Ta et al., 2001b, 2002b; Nguyen et al., 2005). This 40–45 m thick record consists of estuarine channel / tidal river sandy silt, muddy tidal flat/salt marsh, estuarine marine sand and finally open bay mud facies in ascending order. This is consistent with the facies architecture shown in Line 2006-3 (Fig. 4).

To fully understand the evolution of the incised valley fill, a schematic cartoon is shown in Fig. 9 drawn after Allen and Posamentier (1993). Like other incised valleys on the Sunda shelf, this incised valley has probably formed since the shelf exposure caused by the regression (Fig. 9a). Holocene sea-level rise initiated around 19,000 cal yr BP in the South China Sea (Hanebuth et al., 2009). The increased accommodation space was greater than the fluvial sediment flux, thus a transgressive tidal-estuarine facies was formed above the fluvial facies deposited earlier. At the same time, the alluvial plain was continuously built up downstream (Fig. 9b). As the sea-level continuously rose, the alluvial–tidal–delta complex and estuary mouth sand in the form of a tidal inlet migrated up the estuary (Allen and Posamentier, 1993), deeply cutting into the underlying sediment and forming a "ω" shape bottom (Fig. 9c). The local sea-level reached its maximum height around 5500 cal yr BP. Since then, the sea-level has been falling slightly as the MRD began its rapid progradation. The deep cuts formed by tidal inlets were gradually filled with fine materials, which are correlated to the open-bay facies in Core BT2. Here the mud layer, or the open-bay facies, can be treated as a boundary separating an underlying transgressive sequence from the overlying regressive sequence. This is similar to the incised valley fill on the modern Yangtze delta documented by Li et al. (2002). As the delta plain prograded, the estuary gradually moved downstream and formed a thin tidal-estuarine facies shown in Figs. 4 and 9d.

## 6. Summary

High resolution seismic profiles reveal 10–20 m thick deltaic sediments within 30 m water depth surrounding the Mekong River Delta (MRD). Based on the differences in clinoform structure and sediment characters, the subaqueous delta is divided into four zones: Zone I. Mekong River mouth, Zone II. East shore of the Camau Peninsula, Zone III. Cape Camau, and Zone IV. West shore of the Camau Peninsula.

In the last 3000 yr, the evolution of the MRD shows a morphological asymmetry, which is explained by increased wave influence. After the delta body refilled the former bight, the delta edge began to be exposed to longshore coastal currents. Strengthened by the strong NE monsoon, the coastal current transports a large amount of Mekong sediments southwestward. After going through cycles of trapping and resuspension, longshore transported sediments gradually form a large downdrift area and a subaqueous delta. Sediment budget estimation shows that approximately $80 \pm 18\%$ of Mekong sediments have been trapped within the delta area and took part in its rapid progradation over the past 3000 yr.

An incised valley fill is unveiled by seismic profiling, based on which a schematic incised valley fill model since the low sea level stand is proposed.

## Acknowledgement

Financial supports for this joint research come from the International Office of the National Science Foundation (USA), the Office of Naval Research (USA), and the Vietnamese Ministry of Science and Technology. We appreciate the great help from Dr. Elana Leithold and Laurel Childress (NCSU) with the $C_{org}$ and grain size analyses. Two

**Fig. 9.** Schematic cartoon of the development of the incised valley fill (after Allen and Posamentier, 1993) a. The incise valley was formed during low sea-level stand; b. The sea-level rise originated around 19,000–20,000 cal yr BP (Hanebuth et al., 2009), a transgressive tidal-estuarine facies was formed. The alluvial plain was continuously built up in the downstream direction; c. Around 5500 yr BP the local sea-level reached its maximum. As a result, the flood–tidal–delta complex and estuary–mouth sands in the form of a tidal inlet migrated up the estuary, deeply cutting into the underlying sediment and forming a "ω" shape bottom; d. Sea-level has been slightly lowering since the Holocene high sea-level stand. The deep cutting by tidal inlets was gradually filled with fine materials. As the delta plain prograded, the estuary gradually moved downstream and thus formed a thin tidal-estuary depositional layer; e. Sea level curve for the past 15,000 cal yr. (A. Mekong River Delta, gray, Ta et al., 2002a and B. Sunda Shelf, blackline, Hanebuth et al., 2000).

reviewers, Dr. Steven Goodbred Jr. (Vanderbilt University) and one anonymous reviewer, significantly improved the manuscript.

## References


Allen, G.P., Posamentier, H.W., 1993. Sequence stratigraphy and facies model of an incised valley fill: the Gironde Estuary, France. Journal of Sedimentary Research 63 (3), 378–391.

Allison, M.A., Nittrouer, C.A., Kineke, G.C., 1995. Seasonal sediment storage on mudflats adjacent to the Amazon River. Marine Geology 125 (3–4), 303–328.

Bhattacharya, J.P., Giosan, L., 2003. Wave-influenced deltas: geomorphological implications for facies reconstruction. Sedimentology 50, 187–210.

Cattaneo, A., Correggiari, A., Langone, L., Trincardi, F., 2003. The late-Holocene Gargano subaqueous delta, Adriatic shelf: sediment pathways and supply fluctuations. Marine Geology 193 (1–2), 61–91.

Chen, Z., Song, B., Wang, Z., Cai, Y., 2000. Late Quaternary evolution of the sub-aqueous Yangtze Delta, China: sedimentation, stratigraphy, palynology, and deformation. Marine Geology 162 (2–4), 423–441.

Coleman, J.M., Roberts, H.H., 1989. Deltaic coastal wetlands. Geologie en Mijnbouw 68, 1–24.

Correggiari, A., Cattaneo, A., Trincardi, F., 2005. The modern Po Delta system: lobe switching and asymmetric prodelta growth. Marine Geology 222–223, 49–74.

Debenay, J.-P., Luan, B.T., 2006. Foraminiferal assemblages and the confinement index as tools for assessment of saline intrusion and human impact in the Mekong Delta and neighbouring areas (Vietnam). Revue de Micropaleontologie 49 (2), 74–85.

DeMaster, D.J., Pope, R.H., Levin, L.A., Blair, N.E., 1994. Biological mixing intensity and rates of organic carbon accumulation in North Carolina slope sediments. Deep-Sea Research II 41 (4–6), 735–753.

Gagliano, S.M., Mcintire, W.G., 1968. Reports on the Mekong River Delta. Louisiana State University.

Galloway, W.E., 1975. Process framework for describing the morphologic and stratigraphic evolution of deltaic depositional systems. In: Broussard, M.L. (Ed.), Deltas, Models for Exploration. Houston Geological Society, Houston, pp. 87–98.

Geyer, W.R., Hill, P.S., Kineke, G.C., 2004. The transport, transformation and dispersal of sediment by buoyant coastal flows. Continental Shelf Research 24 (7–8), 927–949.

Goodbred, S.L., Kuehl, S.A., 1999. Holocene and modern sediment budgets for the Ganges–Brahmaputra river system; evidence for highstand dispersal to flood-plain, shelf, and deep-sea depocenters. Geology 27 (6), 559–562.

Goodbred, S.L., Kuehl, S.A., 2000. The significance of large sediment supply, active tectonism, and eustasy on margin sequence development: Late Quaternary stratigraphy and evolution of the Ganges–Brahmaputra delta. Sedimentary Geology 133 (3–4), 227–248.

Hanebuth, T.J.J., Stattegger, K., 2004. Depositional sequences on a late Pleistocene–Holocene tropical siliciclastic shelf (Sunda Shelf, southeast Asia). Journal of Asian Earth Sciences 23 (1), 113–126.

Hanebuth, T.J.J., Stattegger, K., Grootes, P.M., 2000. Rapid flooding of the Sunda Shelf: a Late-Glacial sea-level record. Science 288 (5468), 1033–1035.

Hanebuth, T.J.J., Stattegger, K., Saito, Y., 2002. The stratigraphic architecture of the central Sunda Shelf (SE Asia) recorded by shallow-seismic surveying. Geo-Marine Letters 22 (2), 86–94.

Hanebuth, T.J.J., Stattegger, K., Schimanski, A., Ludmann, T., Wong, H.K., 2003. Late Pleistocene forced-regressive deposits on the Sunda Shelf (Southeast Asia). Marine Geology 199 (1–2), 139–157.

Hanebuth, T.J.J., Stattegger, K., Bojanowski, A., 2009. Termination of the Last Glacial Maximum sea-level lowstand: the Sunda-Shelf data revisited. Global and Planetary Change 66 (1–2), 76–84.

Hu, J., Kawamura, H., Hong, H., Qi, Y., 2000. A review on the currents in the South China Sea: seasonal circulation, South China Sea Warm Current and Kuroshio Intrusion. Journal of Oceanography 56, 607–624.

Imamura, F., To, D.V., 1997. Flood and typhoon disasters in Vietnam in the half century since 1950. Natural Hazards 15, 71–87.

Kineke, G.C., Sternberg, R.W., Trowbridge, J.H., Geyer, W.R., 1996. Fluid-mud processes on the Amazon continental shelf. Continental Shelf Research 16 (5–6), 667–696.

Kubicki, A., 2008. Large and very large subaqueous dunes on the continental shelf off southern Vietnam, South China Sea. Geo-Marine Letters 28, 229–238.

Kuehl, S.A., Levy, B.M., Moore, W.S., Allison, M.A., 1997. Subaqueous delta of the Ganges–Brahmaputra river system. Marine Geology 144, 81–96.

Le, T.V.H., Nguyen, H.N., Wolanski, E., Tran, T.C., Haruyama, S., 2007. The combined impact on the flooding in Vietnam's Mekong River delta of local man-made structures, sea level rise, and dams upstream in the river catchment. Estuarine, Coastal and Shelf Science 71 (1–2), 110–116.

Leithold, E.L., Blair, N.E., Perkey, D.W., 2006. Geomorphologic controls on the age of particulate organic carbon from small mountainous and upland rivers. Global Biogeochemical Cycles 20 (GB3022), 1–11.

Li, C., et al., 2002. Late Quaternary incised-valley fill of the Yangtze delta (China): its stratigraphic framework and evolution. Sedimentary Geology 152 (1–2), 133–158.

Liu, J.P., Milliman, J.D., Gao, S., Cheng, P., 2004. Holocene development of the Yellow River's subaqueous delta, North Yellow Sea. Marine Geology 209 (1–4), 45–67.

Liu, J., Saito, Y., Wang, H., Yang, Z., Nakashima, R., 2007a. Sedimentary evolution of the Holocene subaqueous clinoform off the Shandong Peninsula in the Yellow Sea. Marine Geology 236 (3–4), 165–187.

Liu, J.P., et al., 2007b. Flux and fate of Yangtze River sediment delivered to the East China Sea. Geomorphology 85 (3–4), 208–224.

Liu, J.P., et al., 2009. Fate of sediments delivered to the sea by Asian large rivers: long-distance transport and formation of remote alongshore clinothems. SEPM-The Sedimentary Record 7 (4), 4–9.

Milliman, J.D., Meade, R.H., 1983. World-wide delivery of river sediment to the oceans. Journal of Geology 91, 1–21.

Milliman, J.D., Syvitski, J.P.M., 1992. Geomorphic/tectonic control of sediment discharge to the ocean: the importance of small mountainous rivers. Journal of Geology 100 (5), 525–544.

Nguyen, L.V., Ta, T.K.O., Tateishi, M., 2000. Late Holocene depositional environments and coastal evolution of the Mekong River Delta, Southern Vietnam. Journal of Asian Earth Sciences 18 (4), 427–439.

Nguyen, V.L., et al., 2005. Late Quaternary depositional sequences in the Mekong River Delta, Vietnam. In: Chen, Z.Y., Saito, Y., Goodbred, S.L.J. (Eds.), Mega-Deltas of Asia. China Ocean Press, Beijing, pp. 121–127.

Nittrouer, C.A., Kuehl, S.A., DeMaster, D.J., Kowsmann, R.O., 1986. The deltaic nature of Amazon shelf sedimentation. GSA Bulletin 97 (4), 444–458.

Nittrouer, C.A., et al., 1996. The geological record preserved by Amazon shelf sedimentation. Continental Shelf Research 16 (5–6), 817–841.

Roberts, H.H., 1997. Dynamic changes of the Holocene Mississippi River delta plain: The delta cycle. Journal of Coastal Research 13 (3), 691–710.

Roberts, H.H., 1998. Delta switching: early responses to the Atchafalaya River diversion. Journal of Coastal Research 14 (3), 882.

Saito, Y., 2000. Deltas in Southeast and East Asia: their evolution and current problems. In: Mimura, N., Yokoki, H. (Eds.), APN/SURVAS/LOICZ Joint Conference on Coastal Impact of Climate Change and Adaption in the Asia-Pacific Region, Kobe, Japan, pp. 185–191.

Schimanski, A., Stattegger, K., 2005. Deglacial and Holocene evolution of the Vietnam shelf: stratigraphy, sediments and sea-level change. Marine Geology 214 (4), 365–387.

Slingerland, R., Driscoll, N.W., Milliman, J.D., Miller, S.R., Johnstone, E.A., 2008. Anatomy and growth of a Holocene clinothem in the Gulf of Papua. Journal of Geophysical Research 113 (F01S13). doi:10.1029/2006JF000628.

Stanley, D.J., Warne, A.G., 1994. Worldwide initiation of Holocene marine deltas by deceleration of sea-level rise. Science 265 (5169), 228–231.

Swenson, J.B., 2005. Fluviodeltaic response to sea-level perturbations: amplitude and timing of shoreline translation and coastal onlap. Journal of Geophysical Research 110. doi:10.1029/2004JF000208.

Ta, T.K.O., Nguyen, V.L., Kobayashi, I., Tateishi, M., Saito, Y., 2001a. Late Pleistocene–Holocene stratigraphy and delta progradation, the Mekong River delta, South Vietnam. Gondwana Research 4 (4), 799–800.

Ta, T.K.O., Nguyen, V.L., Tateishi, M., Kobayashi, I., Saito, Y., 2001b. Sedimentary facies, diatom and foraminifer assemblages in a late Pleistocene–Holocene incised-valley sequence from the Mekong River Delta, Bentre Province, Southern Vietnam: the BT2 core. Journal of Asian Earth Sciences 20 (1), 83–94.

Ta, T.K.O., et al., 2002a. Sediment facies and Late Holocene progradation of the Mekong River Delta in Bentre Province, southern Vietnam: an example of evolution from a tide-dominated to a tide- and wave-dominated delta. Sedimentary Geology 152 (3–4), 313–325.

Ta, T.K.O., et al., 2002b. Holocene delta evolution and sediment discharge of the Mekong River, southern Vietnam. Quaternary Science Reviews 21 (16–17), 1807–1819.

Ta, T.K.O., Nguyen, V.L., Tateishi, M., Kobayashi, I., Saito, Y., 2005. Holocene delta evolution and depositional models of the Mekong River Delta, Southern Vietnam, River Deltas — concepts, models, and examples. SEPM (Society for Sedimentary Geology) 453–466.

Tamura, T., et al., 2009. Initiation of the Mekong River delta at 8 ka: evidence from the sedimentary succession in the Cambodian lowland. Quaternary Science Reviews Special Theme: Modern Analogues in Quaternary Palaeoglaciological Reconstruction, vol. 28(3–4), pp. 181–260. 327–344.

Walsh, J.P., et al., 2004. Clinoform mechanics in the Gulf of Papua, New Guinea. Continental Shelf Research 24 (19), 2487–2510.

Wolanski, E., Ngoc Huan, N., Trong Dao, L., Huu Nhan, N., Ngoc Thuy, N., 1996. Fine-sediment dynamics in the Mekong River estuary, Vietnam. Estuarine, Coastal and Shelf Science 43 (5), 565–582.

Wolanski, E., Nguyen, H.N., Spagnol, S., 1998. Sediment dynamics during low flow conditions in the Mekong River Estuary, Vietnam. Journal of Coastal Research 14, 472–482.